JOURNAL OF CATALYSIS 95, 473–481 (1985)

Chemisorption Properties of Platinum and Iridium Supported on TiO_2–Al_2O_3 Mixed-Oxide Carriers: Evidence for Strong Metal–Support Interaction Formation

G. B. McVICKER AND J. J. ZIEMIAK

Exxon Research and Engineering Company, Corporate Research Laboratories, Clinton Township, Route 22 East, Annandale, New Jersey 08801

Received December 4, 1984; revised May 6, 1985

Fresh Pt and Ir on Al_2O_3 catalysts reduced at 773 K exhibit high H/M ratios (1 to 2.5) indicative of highly dispersed metal phases. In contrast, TiO_2-supported Pt and Ir catalysts display low H/M ratios (<0.04) following hydrogen reduction at 773 K. The suppressed hydrogen uptakes typically exhibited by TiO_2-based Group VIII metal catalysts result from a strong metal–support interaction (SMSI) and not from a poor metals dispersion. Following reduction at 773 K, the H/M ratios displayed by Pt and Ir catalysts supported on TiO_2–Al_2O_3 mixed-oxide carriers are intermediate in value between those observed on TiO_2 and Al_2O_3 supports. The extent of H_2 uptake suppression is dependent upon the relative TiO_2 and Group VIII metal concentrations on the Al_2O_3 surface. The magnitude of H_2 uptake suppression (and thus SMSI formation) increases at higher TiO_2/Group VIII metal ratios. Higher reduction temperatures and extended reduction times at a given elevated temperature also enhance SMSI formation. Taken together, these results imply that the generation of reduced Group VIII metal–TiO_{2-x} species on the Al_2O_3 surface may be responsible for the SMSI effect.

1. INTRODUCTION

Over the past several years, a new family of supported metal catalysts has been developed by a large number of investigators. Through the early efforts of Tauster *et al.*, a number of ceramic carriers which induce strong interactions with a supported metal phase were identified (*1*, *2*). Systems exhibiting strong metal–support interactions have been designated SMSI catalysts. Representative carriers include TiO_2, V_2O_3, Ta_2O_5, and Nb_2O_5, and typical metals include the Group VIII series (*2*).

Group VIII metal SMSI catalysts are phenomologically characterized by suppressed H_2 and CO chemisorption capacities and in certain cases by a resistance to sintering of the Group VIII metal component at elevated reduction or oxidation temperatures (*1*). The presence of well-dispersed Group VIII metal phases in SMSI catalysts has been established by X-ray line broadening, transmission electron microscopy (TEM), and O_2 chemisorption measurements (*1*, *3–5*). The essential absence of H_2 and CO chemisorption is a consequence of SMSI and not the result of a poorly dispersed Group VIII metal component. The existence of strong metal–support interactions has also been inferred from experiments in which bulk Group VIII metals were found to disperse on TiO_2 following calcination of a physical mixture of the two components at elevated temperatures.

Group VIII metal SMSI catalysts have also been reported to alter numerous catalytic reaction patterns (*6–10*). An example of such reactivity modification is ethane hydrogenolysis. The hydrogenolysis activities of Pt and Ir supported on Al_2O_3, SiO_2, and TiO_2 carriers are compared in Table 1. The hydrogenolysis activities of Pt and Ir on TiO_2 are approximately an order of magnitude lower than the same metals supported on either Al_2O_3 or SiO_2. Suppressed hydrogenolysis, as well as hydrogenation, activi-

0021-9517/85 $3.00

TABLE 1

Ethane Hydrogenolysis: The Effect of Support on Catalyst Activity[a]

Catalyst	E_a[b]	Rate[c] (523 K)
2% Pt/Al_2O_3	55	5.7×10^9
10% Pt/SiO_2[d]	54	2.2×10^9
2% Pt/TiO_2	55	1.3×10^8
2% Ir/Al_2O_3	51	5.2×10^{13}
10% Ir/SiO_2[d]	36	5.8×10^{13}
2% Ir/TiO_2	46	2.9×10^{12}

[a] Ethane hydrogenolysis was carried out at 101 kPa with partial pressures of He, H_2, and ethane of 78, 20, and 3 kPa, respectively. 2.0 g of catalyst was employed and reduced at 673 K with 20% H_2/He (500 cm^3/min) for 1.0 hr prior to use.

[b] E_a = apparent activation energy (kcal/mole).

[c] Reaction rates (molecules/sec/cm^2).

[d] Abstracted from Sinfelt (*30*).

ties appear to be a general feature of SMSI catalysts.

Although SMSI carriers successfully stabilize some Group VIII metals against reductive and oxidative sintering and beneficially modify certain catalytic conversions (e.g., reduce hydrogenolysis, lower methane made under Fischer–Tropsch synthesis conditions), they do suffer several limitations. Chief among these is that, under typical reaction temperatures (570–870 K), SMSI carriers often experience reductions in surface area. Following thermal treatment BET surface areas of 25 m^2/g or less are exhibited by many of these carriers. The loss in carrier surface area potentially reduces the quantity of Group VIII metals which can be maintained in a well-dispersed state. Surface-area collapse may also encapsulate a significant quantity of the Group VIII metal component within the carrier pore structure and thereby render the active metal unavailable for catalytic utilization. Finally, a loss in surface area can significantly reduce the concentration of Group VIII metals which can be retained on the carrier surface.

In an attempt to stabilize the surface area of SMSI carriers, preparative techniques were employed which place a SMSI phase on the surface of a non-SMSI support. The preparative technique involves the reaction of a hydrolyzable complex of titanium (e.g., $TiCl_4$, $Ti(OC_3H_7)_4$) with the hydroxyl groups present on the surface of supports such as Al_2O_3 and SiO_2 (*11*). The generation of a supported TiO_2 phase is completed by air calcining the partially hydrolyzed surface complex at an elevated temperature. Supported TiO_2 carriers display high, thermally stable BET surface areas and exhibit only Al_2O_3 or SiO_2 X-ray diffraction patterns. The absence of X-ray diffraction patterns from the supported TiO_2 component suggests that this phase is either well dispersed over the Al_2O_3 or SiO_2 surface or that it is amorphous.

Preliminary chemisorption studies indicated that Group VIII metals supported on TiO_2–Al_2O_3 carriers exhibit H_2 chemisorption uptakes intermediate between those found on TiO_2 and Al_2O_3. To better quantify the effects changes in the TiO_2 Group VIII-metal ratio have upon chemisorption properties and relative oxidative sintering stabilities of Group VIII metals, a study of Pt and Ir catalysts on TiO_2, Al_2O_3, and TiO_2–Al_2O_3 carriers was undertaken. The investigative probes included X-ray diffraction, H_2 chemisorption, and TEM measurements. This paper summarizes the results of these studies.

2. EXPERIMENTAL

Catalysts. A series of 0.3–2 wt% Pt and Ir catalysts was prepared on TiO_2, Al_2O_3, and TiO_2–Al_2O_3 supports by incipient wetness impregnation. Analyzed aqueous solutions of chloroplatinic and chloroiridic acids (0.1 g metal/cm^3) were employed. The impregnates were dried in dry air for 16 hr at 393 K and then mildly calcined in dry air at 543 K for an additional 4.0 hr. Metal analyses were found in all cases to be in good agreement with the nominal values (*12*). TiO_2 supports were used as supplied by either Degussa or Cabot Corporation.

The physical properties of both of these materials are similar (*1*). TiO_2–Al_2O_3 mixed-oxide supports were prepared by the incipient wetness impregnation of dried η-Al_2O_3 powders (192 m^2/g) with heptane solutions of $TiCl_4$ under a nitrogen atmosphere in a drybox enclosure. Heptane was removed with reduced pressure (10^{-3} Torr). A surface TiO_2 phase was produced by air calcining the partially hydrolyzed titanium chloride at 823 K for 16 hr. TiO_2–Al_2O_3 supports were also prepared by the incipient wetness impregnation of dry γ-Al_2O_3 (178 m^2/g) with toluene solutions of titanium isopropoxide ($Ti(OC_3H_7)_4$) under nitrogen. Toluene was removed with reduced pressure. A surface TiO_2 phase was prepared by allowing the isopropoxide to slowly hydrolyze in air overnight followed by air calcining at 823 K for 16 hr. The air-calcined TiO_2–Al_2O_3 mixed-oxide supports are white.

Chemisorption measurements. Hydrogen chemisorption studies were performed with a conventional glass-vacuum system (*13*). The system incorporated an oil-diffusion pump backed by a mechanical pump with liquid-nitrogen traps on the inlet and outlet of the diffusion pump. Ultimate dynamic vacua of about 10^{-7} Torr were obtainable. Pressure measurements during chemisorption studies were made with a Texas Instruments precision pressure gauge. Samples of 1–4 g, sieved to 20–40 mesh size, were placed in flow-through cells made of quartz. Samples were reduced at selected temperatures under hydrogen (500 cm^3/min) *in situ* for various times. The reduced samples were allowed to cool 50 K below the reduction temperature under hydrogen and evacuated at this temperature for 0.5 hr. The sample was then cooled under dynamic vacuum to room temperature. Longer evacuation times did not affect the chemisorption results. Hydrogen uptakes were determined at 298 ± 2 K on the reduced and evacuated samples. Typically, 0.5 hr was allowed for each uptake point. H/M ratios were calculated by assuming that H_2 uptakes at zero pressure of H_2 corresponded to saturation coverage of the metal. These uptakes were determined by extrapolation of the high-pressure linear portion of the isotherm as described by Benson and Boudart and Wilson and Hall (*14, 15*). BET surface-area measurements were determined with argon at liquid-nitrogen temperature (*16*). A value of 0.146 nm^2 was assumed for the area of an argon atom and a value of 210 Torr was used for P_0. Hydrogen of 99.95% purity was passed through a Deoxo unit (Engelhard Industries, Inc.), a 5-Å molecular-sieve drying trap, an Oxy-trap (Alltech Associates, Arlington Heights, Ill.) to remove last traces of oxygen, and finally through a liquid-nitrogen trap before being admitted to the catalyst for reductions or chemisorption measurements.

Sintering treatments. Oxidative calcinations of catalysts under 101 kPa (760 Torr) total pressure and various temperatures were carried out by one of the following procedures: (i) calcining under dry air in a muffle furnace, (ii) calcining under dry air or 20% O_2/He flowing at 500 cm^3/min in a quartz tube furnace, or (iii) calcining under dry air (200–500 cm^3/min) in a quartz gas-adsorption cell. Catalysts were reduced prior to oxidative calcination treatments.

X-Ray diffraction measurements. A Philips Electronics X-ray diffractometer (XRG-3000) with nickel-filtered Cu$K\alpha$ radiation was used for X-ray diffraction studies. Metal and metal-oxide crystallite sizes were calculated from line-broadening measurements, as described elsewhere (*17*). The 400 diffraction line of Al_2O_3 was employed as an internal standard when the relative extent of Group VIII-metal sintering was determined.

Cyclohexene isomerization. Cyclohexene conversions were carried out over Al_2O_3 and TiO_2–Al_2O_3 supports in a 25-cm^3 fixed-bed stainless-steel reactor to ascertain the relative acidity of these materials (*18*). Skeletal isomerization of cyclohexene to a mixture of isomeric (*1*, *3*, *4*)-methylcyclopentenes was carried out at 623 K under 1380 kPa total pressure. The space velocity was 25 WHW and the H_2/cyclohexene ratio was held at 2.3. Preliminary studies established that under these conditions no appreciable mass or pore-volume diffusion limitations were encountered with these materials. Product analyses were carried out by on-line GC measurements employing a 300-ft. squalene capillary column in conjunction with flame-ionization detection.

Acidity measurements. The acidities of TiO_2, Al_2O_3, and TiO_2–Al_2O_3 supports were determined by titration of the solids with a standardized *n*-butylamine/benzene solution in the presence of a series of Hammett indicators (*19*, *20*). Prior to acidity measurements the supports were calcined under dry air at 773 K.

TEM measurements. Electron microscopy studies were performed on a Philips EM300 transmission electron microscope as described by Prestridge and Yates (*21*).

TABLE 2

Selected Properties of TiO_2, Al_2O_3, and TiO_2–Al_2O_3 Supports

Support	BET surface area (m^2/g)	Total acidity[a] $H_0 \leq -3.0$ ($\pm$0.1 μmole/m^2)	Strong acidity $H_0 \leq -8.2$ ($\pm$0.1 μmole/m^2)
η-Al_2O_3	192	2.5	1.7
γ-Al_2O_3	178	2.5	1.7
TiO_2[b]	60	1.1	0
2.1% TiO_2–Al_2O_3[c]	179	1.8	1.8
16.7% TiO_2–Al_2O_3[c]	161	2.0	1.7
1.7% TiO_2–Al_2O_3[d]	154	2.2	2.1
8.3% TiO_2–Al_2O_3[d]	159	2.0	2.0
16.7% TiO_2–Al_2O_3[d]	153	2.1	2.1

[a] Total acidity includes sites of strengths ≤ -8.2, ≤ -5.6, and ≤ -3.0 H_0 as determined by *n*-butylamine titration in the presence of a series of Hammett indicators: $H_0 \leq -8.2$, anthraquinone indicator (acidic form requires 90% H_2SO_4); $H_0 \leq -5.6$, benzalacetophenone indicator (acidic form requires 71% H_2SO_4); $H_0 \leq -3.0$, dicinnamalacetone indicator (acidic form requires 48% H_2SO_4).

[b] Strongest acid sites are $H_0 \leq -5.6$.

[c] Prepared by $TiCl_4$ impregnation of η-Al_2O_3 (mixed oxide prepared by calcining at 823 K under air for 16 hr).

[d] Prepared by $Ti(OC_3H_7)_4$ impregnation of γ-Al_2O_3 (mixed oxide prepared by calcining at 823 K under air for 16 hr).

3. RESULTS AND DISCUSSION

General Properties of TiO_2–Al_2O_3 Supports

Selected properties of the TiO_2, Al_2O_3, and TiO_2–Al_2O_3 supports used in this study are summarized in Table 2. TiO_2–Al_2O_3 mixed-oxide supports retain BET surface areas in the range of 150–180 m^2/g even after calcining at 870–1070 K for extended times. Air-calcined TiO_2–Al_2O_3 samples are devoid of TiO_2 X-ray diffraction lines. The absence of a TiO_2 X-ray pattern suggests that this phase is well dispersed over the Al_2O_3 surface. In the case of a 16.7% TiO_2–Al_2O_3 carrier, selected area electron microscopic examination failed to reveal the presence of TiO_2. This result indicates that TiO_2 is present in crystallites less than 1.0 nm in diameter and moreover that such crystallites must be highly dispersed over the Al_2O_3 surface. In general, the surface hydrolysis method of preparation favors the formation of well-dispersed TiO_2 phases. In contrast to TiO_2–Al_2O_3 carriers, air calcination of TiO_2 at 870 K results in a decrease in BET surface area from 60 to 18 m^2/g. Thermally stable TiO_2–Al_2O_3 mixed-oxide carriers, thus, offer the potential of providing a well-dispersed TiO_2 surface phase at which a SMSI may occur with a supported Group VIII metal.

n-Butylamine titrations on TiO_2–Al_2O_3 carriers were performed to establish if a supported TiO_2 phase modifies that acidity of the Al_2O_3 support. The total acidity of TiO_2 per unit surface area is about 60% lower than that of η- or γ-Al_2O_3 (see Table 2). Unlike the transitional aluminas, TiO_2 does not possess acidic centers stronger than $H_0 = -5.6$. Mixed-oxide TiO_2–Al_2O_3 supports, however, exhibit acidities comparable to that of Al_2O_3. An eightfold increase in the supported TiO_2 concentration did not measurably decrease the number of strong acid sites ($H_0 \leq -8.2$). We have estimated that 2.1 and 16.7% TiO_2 phases dispersed monoatomically as TiO_2 would occupy 6.2 and 49.5%, respectively, of the Al_2O_3 surface. Acidity retention demon-

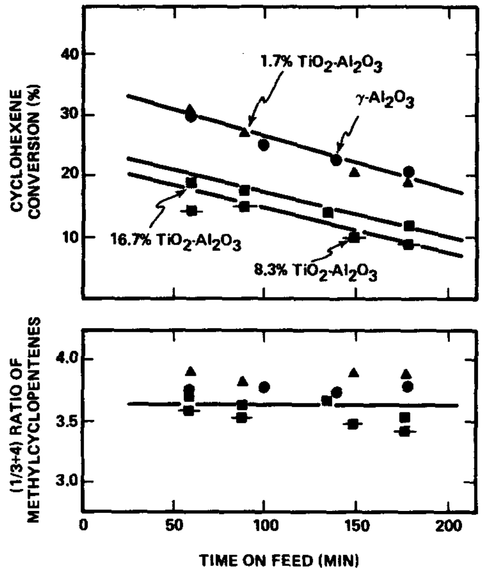

FIG. 1. Isomerization of cyclohexene over TiO_2–Al_2O_3 mixed-oxide supports. Run conditions: 623 K, 1380 kPa, H_2/cyclohexene = 2.3, WHW = 25.

strated by the TiO_2–Al_2O_3 carriers implies that either TiO_2 does not interact with the Al_2O_3 acid sites which trigger Hammett indicators or that new acid centers are generated at an Al_2O_3–TiO_2 interface. Further, the choice of Ti precursor does not appear to affect the number or the distribution of acid sites on TiO_2–Al_2O_3 supports.

The retention of acidity on the TiO_2–Al_2O_3 mixed-oxide carriers suggested by the *n*-butylamine titrations was confirmed by cyclohexene isomerization studies. The results of these studies are presented in Fig. 1. As measured by the quantity of cyclohexene isomerized, 8.3 and 16.7% TiO_2–Al_2O_3 supports prepared via a $Ti(OC_3H_7)_4$ precursor are 30 to 40% less active isomerization catalysts than γ-Al_2O_3. Thus cyclohexene isomerization is a more sensitive surface acidity probe than *n*-butylamine titration, since the latter method indicated little (about 10%) acidity differences between these materials and γ-Al_2O_3. A 1.7% TiO_2–Al_2O_3 carrier, also prepared via $Ti(OC_3H_7)_4$, exhibits an isomerization activity comparable to that of γ-Al_2O_3. This result indicates that low TiO_2 concentrations do not adversely effect the acidity of γ-Al_2O_3. TiO_2–Al_2O_3 catalysts prepared via impregnation of $TiCl_4$ are about 30% more active cyclohexene isomerization catalysts than those prepared using a $Ti(OC_3H_7)_4$ precursor. This difference arises from the retention of the chloride ion (~0.6 wt%) on the $TiCl_4$-prepared mixed oxides. Upon the addition of 0.6 wt% Cl, the isomerization activity of γ-Al_2O_3 is also increased by about 30%. The catalysts compared in Fig. 1 exhibited essentially equivalent selectivities as measured by the 1/(3 + 4) ratio of isomeric methylcyclopentenes. The measured ratios are close to the 3.6 equilibrium value expected at 623 K (*22*).

Chemisorption Studies

A number of Pt and Ir catalysts supported on TiO_2, Al_2O_3, and TiO_2–Al_2O_3 carriers have been characterized by H_2 chemisorption measurements. A sampling of these measurements is presented in Table 3. Catalysts were routinely reduced under H_2 (500 cm^3/min) at 773 K then evacuated at 723 K for 0.5 hr prior to H_2 chemisorption measurements at 298 K. Calcined samples were treated under 20% O_2/He (500 cm^3/min) at 773 K for 4.0 hr and then subjected to the reduction conditions outlined above.

Al_2O_3 Supported Catalysts

Fresh 0.3–2% Pt on Al_2O_3 catalysts exhibit H/Pt values near unity. Such values are normal for well-dispersed platinum catalysts (*23, 24*). Pt/Al_2O_3 catalysts calcined under oxygen at 773 K retain high surface areas. Temperatures in excess of 900 K are generally required to appreciably sinter Al_2O_3-supported Pt catalysts (*25*). Fresh Ir/Al_2O_3 catalysts exhibit H/Ir values in excess of unity. H/Ir values in the range 1.8 to 2.6 are typically obtained for fresh 0.3 to 2% Ir catalysts (*26, 27*). Multiple absorbate bonding has been shown to be a property of highly dispersed iridium particles and not of hydrogen spillover (*26*). Ir/Al_2O_3 catalysts oxidatively calcined at 773 K for 4.0 hr are, in contrast to Pt/Al_2O_3 catalysts, readily

TABLE 3

Chemisorption Measurements[a]

Group VIII metal	Support (%)		H/M	
	Al_2O_3	TiO_2	Fresh	Calcined[b]
2% Pt	100	—	1.0	1.0
1% Pt	100	—	1.2	1.2
0.3% Pt	100	—	1.2	1.2
2% Ir	100	—	1.9	0.38[c]
1% Ir	100	—	2.1	0.28[c]
0.3% Ir	100	—	2.6	0.48[c]
2% Pt	—	100	0.01	0.02
0.3% Pt	—	100	0.04	0.03
2% Ir	—	100	0.02	0.01
0.3% Ir	—	100	0.01	0.01
0.3% Pt	98.3	1.7	1.2	1.2
0.3% Pt	97.9	2.1	1.1	1.1
0.3% Pt	83.3	16.7	0.63	0.62
2% Pt	83.3	16.7	0.44	0.46
0.3% Ir	97.9	2.1	2.5	1.2[c]
0.3% Ir	83.3	16.7	1.4	0.23[c]
2% Ir	83.3	16.7	0.74	0.16[c]

[a] Catalysts reduced 2 hr at 773 K under H_2 (500 cm^3/min) then evacuated at 723 K for 0.5 hr prior to chemisorption measurements at 298 ± 2 K.

[b] Calcined under 20% O_2/He (500 cm^3/min) at 773 K for 4.0 hr then subjected to conditions outlined in (a) above.

[c] Calcined samples demonstrated IrO_2 X-ray diffraction patterns indicating substantial crystallite growth (15- to 25-nm particles).

sintered. The sintering process is accompanied by a sharp decrease in the respective H/Ir values and by the appearance of IrO_2 X-ray diffraction lines in the calcined samples (*25, 28, 29*).

TiO_2-Supported Catalysts

Platinum and iridium supported on TiO_2 demonstrate extremely suppressed hydrogen uptakes following reduction at 773 K. H/M values for these catalysts are typically less then 0.02. The suppression of H_2 chemisorption is essentially independent of metal loading. The inability of these catalysts to chemisorb hydrogen at room temperature is a consequence of SMSI and is not the result of poorly dispersed Group VIII-metal phases (*1*). The apparent H/M values of TiO_2-supported Pt and Ir catalysts are not altered upon calcining under oxygen at 773 K. Both fresh and calcined TiO_2-based catalysts are devoid of X-ray diffraction patterns due to sintered metal (Pt, Ir) or metal-oxide (IrO_2) phases. Alumina-supported Pt or Ir catalysts displaying H/M values near 0.02 would, in contrast, display X-ray lines indicative of large, 40- to 60-nm metal crystallites. The absence of X-ray diffraction lines in calcined TiO_2-supported catalysts indicates that the metal crystallites are less than 5.0 nm in diameter (*17*).

The extent of H_2 chemisorption suppression in TiO_2-based, SMSI catalysts is dependent upon reduction temperature. This dependency is presented in Fig. 2. The curves show that the H/M values of both Pt and Ir are markedly lowered at higher reduction temperatures. Following a 573 K reduction, Pt and Ir are only partially in the SMSI state. The nearly complete suppression of hydrogen chemisorption at higher reduction temperatures suggests the formation of a reduced surface species of some kind. The generation of a Group VIII metal–TiO_{2-x} species has been implicated as a possible reduced metal phase (*1, 2, 5*). The SMSI state established by reduction at 773 K is destroyed by calcining in air at temperatures above 673 K. Subsequent reduction of the calcined catalyst at 573 K generates a system which exhibits an H/M

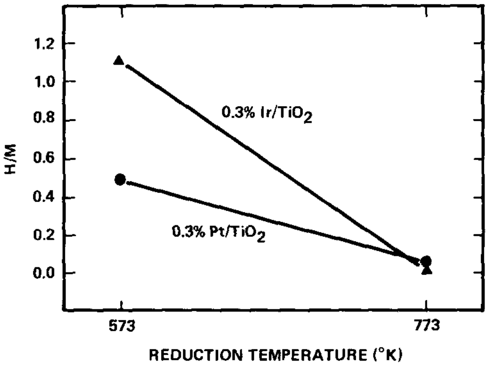

FIG. 2. The effect of reduction temperature on the hydrogen uptakes of TiO_2-supported 0.3% Pt and 0.3% Ir catalysts. Reduction conditions: 573 or 773 K, H_2 (500 cm^3/min), 2.0 hr.

TABLE 4

Sintering of 2% Iridium Catalysts[a]

Support (%)		IrO_2 crystallite size[b] (nm)	Relative sintering[c] (%)
Al_2O_3	TiO_2		
—	100	—	0
100	—	18–22	100
83.3	16.7	18–22	85–90

[a] Following an H_2 reduction at 773 K, the catalysts were calcined under 20% O_2/He (500 cm^3/min) at 773 K for 4.0 hr.

[b] Calculated from the half-width of the IrO_2 diffraction line at $2\Theta = 53.8°$.

[c] Calculated from the relative peak areas of the IrO_2 diffraction line at $2\Theta = 28°$ and the Al_2O_3 (400) diffraction line.

value similar in magnitude to that obtained by reducing the fresh catalyst at the lower temperature. The destruction of the SMSI state by oxidation supports the contention that a reduced Group VIII metal–Ti surface species is responsible for the suppression of H_2 chemisorption in Pt and Ir on TiO_2 catalysts.

TiO_2–Al_2O_3-Supported Catalysts

The H/Pt values of fresh Pt on TiO_2–Al_2O_3 catalysts (see Table 3) reduced at 773 K decrease from unity at higher TiO_2/Pt ratios. This may result either from a lower initial platinum dispersion (2- to 4-nm Pt crystallites versus 1.0-nm Pt crystallites) or from partial SMSI formation between the supported TiO_2 phase and a fraction of the platinum component. It is reasonable to assume that the latter effect would be favored in catalysts possessing higher TiO_2/Pt ratios. As found for Pt/Al_2O_3 catalysts, the apparent H/Pt values of these catalysts are not lowered by oxidative calcination at 773 K.

H/Ir values for fresh Ir on TiO_2–Al_2O_3 catalysts were also found to decrease with increasing TiO_2/Ir ratios. Thus the chemisorption behavior of Pt and Ir supported on TiO_2–Al_2O_3 carriers is dependent upon the relative metal and TiO_2 concentrations on the Al_2O_3 surface. In contrast to Pt/TiO_2–Al_2O_3 and Ir/TiO_2 catalysts, Ir/TiO_2–Al_2O_3 catalysts were sintered upon calcining under oxygen at 773 K (see Table 4). The relative extent of Ir sintering on TiO_2–Al_2O_3 carriers is comparable to that observed for Ir/Al_2O_3 catalysts. Thus, TiO_2–Al_2O_3 mixed-oxide carriers function as SMSI supports under reducing conditions but, in contrast to TiO_2, do not stabilize Ir against oxidative agglomeration. An attempt was made to redisperse a sintered 2% Ir/16.7% TiO_2–Al_2O_3 catalyst by reducing under hydrogen at 973 K for several hours. Such conditions, it was reasoned, might generate mobile Ir species which would be subsequently trapped by well-dispersed, reduced, surface TiO_2 centers. The result of such a capture would possibly by the formation of a more highly dispersed, Ir–TiO_{2-x} surface species. Redispersion, however, by this procedure was not successful.

The Effect of Reduction Temperature

The effect of reduction temperature on the H_2 chemisorption properties of 0.3% Pt catalysts on Al_2O_3 and TiO_2–Al_2O_3 carriers is summarized in Fig. 3. The curves were generated by sequentially reducing the three catalysts under H_2 (500 cm^3/min) at the stated temperatures for 2.0 hr. H_2 che-

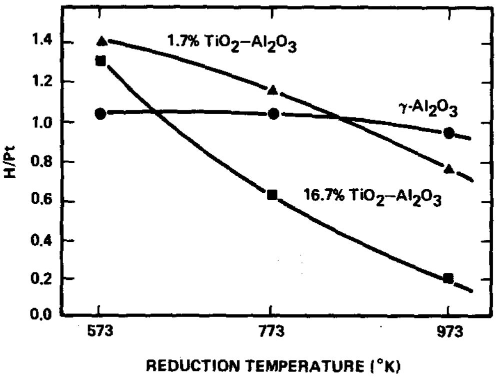

FIG. 3. The effect of reduction temperature on the hydrogen uptakes of 0.3% Pt catalysts on Al_2O_3 and TiO_2–Al_2O_3 supports. Reduction conditions: 573, 773, and 973 K, H_2 (500 cm^3/min), 2.0 hr.

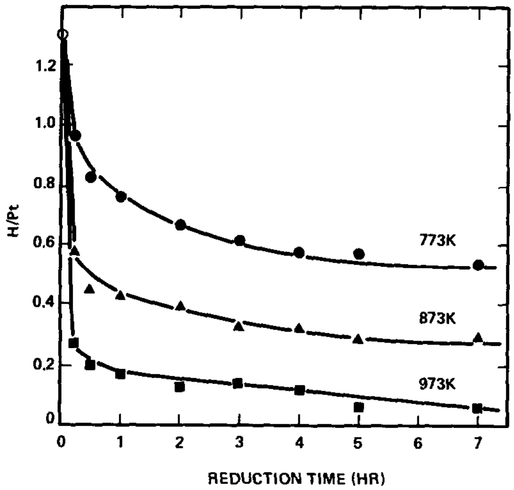

FIG. 4. The effect of extended reduction times on the hydrogen uptakes of a 0.3% Pt/16.7% TiO_2–Al_2O_3 catalyst. Reduction conditions: 773, 873, and 973 K, H_2 (500 cm^3/min), 0.25 to 7.0 hr.

misorption at 298 K was then measured after each reduction step.

The H/Pt ratio of 0.3% Pt/Al_2O_3 was not altered by increasing the reduction temperature from 573 to 973 K. The two TiO_2–Al_2O_3-supported 0.3% Pt catalysts, however, exhibit increasingly lower H/Pt values at higher reduction temperatures. The largest decrease in H/Pt value occurred in the catalyst containing the higher TiO_2/Pt ratio. The suppression of hydrogen uptake is consistent with the onset of SMSI. The data suggests that SMSI formation is favored by higher TiO_2/Pt ratios and by higher reduction temperatures. At the higher reduction temperature, the 0.3% Pt/16.7% TiO_2–Al_2O_3 catalyst demonstrated an H/Pt value approaching that exhibited by Pt/TiO_2 catalysts in the SMSI state. As was found for Pt/TiO_2 catalysts, the SMSI state in TiO_2–Al_2O_3-supported 0.3% Pt catalysts was broken by calcining under 20% O_2/He (500 cm^3/min) at 723 K for 4.0 hr. Upon breakage of the SMSI and then reducing at a lower temperature, a substantial increase in the H/Pt value occurred. Following a 573 K reduction, the calcined Pt/TiO_2–Al_2O_3 catalysts regained 60–70% of their initial (non-SMSI state) H/Pt values. No X-ray evidence for the sintering of Pt was observed in any of these catalysts.

The Effect of Reduction Time

The effect of extended reduction times on the H_2 chemisorption properties of a 0.3% Pt/16.7% TiO_2–Al_2O_3 catalyst is presented in Fig. 4. The catalyst was sequentially reduced under H_2 (500 cm^3/min) for the times and temperatures listed on the curve. At a given reduction temperature, a substantial decline in the H/Pt value was observed over a 7-hr period. The initial H/Pt of 1.31 ($t = 0$) was obtained on a sample reduced at 573 K for 2.0 hr. At this temperature, the Pt component is not in a SMSI state and displays normal H_2 chemisorption behavior. At higher reduction temperatures, the major decrease in hydrogen uptake occurs within the first hour of treatment. The initial rapid loss in H_2 chemisorption capacity followed by a more gradual decline in H_2 uptake at a given temperature suggests that the migration of Pt to a reduced TiO_2 center may be kinetically controlling the rate of SMSI formation. Reduction for 7 hr at 973 K was required to completely suppress H_2 chemisorption. A complicating factor present in the Pt/TiO_2–Al_2O_3 system may be the reducibility of the TiO_2 centers. A TiO_2 site on an Al_2O_3 matrix may be more difficult to reduce than pure TiO_2. Such an effect may partially account for the higher reduction temperatures required to impart SMSI formation in Pt/TiO_2–Al_2O_3 catalysts. Electron micrographs of the 16.7% TiO_2–Al_2O_3 support and the 0.3% Pt/16.7% TiO_2–Al_2O_3 catalyst each reduced at 973 K for 7 hr were recorded. No evidence for the presence of a TiO_2 phase was observed in either sample. The platinum-containing catalyst exhibited thin, faceted Pt crystallites having maximum diameters of 1.5 nm. The average Pt diameter for the observable crystallites was near 1.0 nm. The electron micrographs thus support the suggestion that the suppression of H_2 chemisorption in Pt/TiO_2–Al_2O_3 catalysts results from the SMSI formation and not from agglomeration of the Pt component.

4. SUMMARY

A number of Pt and Ir catalysts supported on TiO_2, Al_2O_3, and TiO_2–Al_2O_3 carriers were studied by H_2 chemisorption, X-ray diffraction, and TEM measurements. Fresh Pt and Ir catalysts supported on Al_2O_3 exhibit high H/M values indicative of well-dispersed noble metal components. The surface areas of Pt/Al_2O_3 catalysts are not lowered by oxidative calcination at 773 K. Ir/Al_2O_3 catalysts are, in contrast, sintered by such treatments.

Fresh Pt and Ir on TiO_2 catalysts display extremely low (<0.02) H/M values. Suppressed hydrogen uptakes result from SMSI formation and not from poorly dispersed metal phases. TiO_2-supported Pt and Ir catalysts are not sintered by calcining under oxygen at 773 K.

The H/M ratios of fresh TiO_2–Al_2O_3-supported Pt and Ir catalysts are intermediate in value to those found on TiO_2 and Al_2O_3 supports. The extent of hydrogen uptake suppression depends upon the relative Group VIII-metal and TiO_2 concentrations on the Al_2O_3 carrier. The magnitude of H_2 chemisorption suppression increases with increasing TiO_2/Group-VIII metal ratio. This systematic trend implies that interaction between the supported Group VIII metal and TiO_2 components is favored at higher TiO_2/Group VIII-metal ratios. Higher reduction temperatures and increased reduction times also enhance the rate of loss of H_2 chemisorption (SMSI formation). Oxidative sintering of Ir catalysts on TiO_2–Al_2O_3 supports is comparable to that observed for Ir/Al_2O_3 catalysts.

ACKNOWLEDGMENTS

The authors thank Dr. L. L. Murrell for measuring the acidity of the various supports. Special thanks are extended to Mr. P. J. Collins and Mr. N. C. Dispenziere, Jr., for their experimental assistance.

REFERENCES

1. Tauster, S. J., Fung, S. L., and Garten, R. L., *J. Amer. Chem. Soc.* **100,** 170 (1978).
2. Tauster, S. J., and Fung, S. L., *J. Catal.* **55,** 29 (1978).
3. Baker, R. T. K., Prestridge, E. B., and Garten, R. L., *J. Catal.* **56,** 390 (1979).
4. Smith, J. S., Thrower, P. A., and Vannice, M. A., *J. Catal.* **68,** 270 (1981).
5. Chen, B., and White, J. M., *J. Phys. Chem.* **86,** 3534 (1982).
6. Vannice, M. A., and Garten, R. L., *J. Catal.* **56,** 236 (1979).
7. Wang, S-Y., Moon, S. H., and Vannice, M. A., *J. Catal.* **71,** 167 (1981).
8. Meriaudeau, P., Ellestad, O. H., Dufaux, M., and Naccache, C., *J. Catal.* **75,** 243 (1982).
9. Burch, R., and Flambard, A. R., *J. Chem. Soc., Chem. Commun.*, 123 (1981).
10. Vannice, M. A., Twu, C. C., and Moon, S. H., *J. Catal.* **79,** 70 (1983).
11. Chien, J. C. W., *J. Catal.* **23,** 71 (1971).
12. Analyses were performed by the Analytical and Information Division, Exxon Research and Engineering Company, Linden, N.J.
13. Sinfelt, J. H., and Yates, D. J. C., *J. Catal.* **8,** 82 (1967).
14. Benson, J. E., and Boudart, M., *J. Catal.* **4,** 704 (1965).
15. Wilson, G. R., and Hall, W. K., *J. Catal.* **17,** 190 (1970).
16. Brunauer S., Emmett, P. H., and Teller, E., *J. Amer. Chem. Soc.* **60,** 309 (1938).
17. Klug, H. P., and Alexander, L. E., "X-Ray Diffraction Procedures for Polycrystalline and Amorphous Materials," 2nd ed., p. 687. Wiley, New York, 1974.
18. Pines, H., and Haag, W. O., *J. Amer. Chem. Soc.* **83,** 2847 (1961).
19. Benesi, H. A., *J. Phys. Chem.* **61,** 970 (1957).
20. Bertolacini, R. J., *Anal. Chem.* **35,** 599 (1963).
21. Prestridge, E. B., and Yates, D. J. C., *Nature (London)* **234,** 345 (1971).
22. Herling, J., Shabtai, J., and Gil-Av, E., *J. Amer. Chem. Soc.* **87,** 4107 (1965).
23. Gruber, H. L., *J. Chem. Phys.* **66,** 48 (1962).
24. Spenadel, L., and Boudart, M., *J. Chem. Phys.* **64,** 204 (1960).
25. McVicker, G. B., Garten, R. L., and Baker, R. T. K., *J. Catal.* **54,** 129 (1978).
26. McVicker, G. B., Baker, R. T. K., Garten, R. L., and Kugler, E. L., *J. Catal.* **65,** 207 (1980).
27. Krishnamurthy, S., Landolt, G. R., and Schoennagel, H. J., *J. Catal.* **78,** 319 (1982).
28. Garten, R. L., and Sinfelt, J. H., *J. Catal.* **62,** 127 (1980).
29. Sinfelt, J. H., and Via, G. H., *J. Catal.* **56,** 1 (1979).
30. Sinfelt, J. H., *Catal. Rev.* **3,** 175 (1969).